Omega-P, Inc.
291 Whitney Avenue – Suite 401
New Haven, CT 06511

DIELECTRIC WAKE FIELD RESONATOR ACCELERATOR MODULE

J. L. Hirshfield, Principal Investigator
tel: (203) 789-1164, e-mail: jay@omega-p.com

ABSTRACT: Results are presented from experiments, and numerical analysis of wake fields set up by electron bunches passing through a cylindrical or rectangular dielectric-lined structure. These bunches excite many TM-modes, with E_z components of the wake fields sharply localized on the axis of the structure periodically behind the bunches. The experiment with the cylindrical structure, carried out at ATF Brookhaven National Laboratory, used up to three 50 MeV bunches spaced by one wake field period (21 cm) to study the superposition of wake fields by measuring the energy loss of each bunch after it passed through the 53-cm long dielectric element. The millimeter-wave spectrum of radiation excited by the passage of bunches is also studied. Numerical analysis was aimed not only to simulate the behavior of our device, but in general to predict dielectric wake field accelerator performance. It is shown that one needs to match the radius of the cylindrical dielectric channel with the bunch longitudinal rms-length to achieve optimal performance.

———————

Key words: dielectric accelerator, wake fields, wake field accelerator

November 6, 2013

EXPERIMENTAL AND NUMERICAL STUDIES OF DIELECTRIC WAKE FIELD ACCELERATION DEVICES*

S.V. Shchelkunov[#], J.-M. Fang, T.C. Marshall, Columbia University, New York, NY 10027
J.L. Hirshfield, Yale University, and Omega-P, Inc., New Haven, CT 06511

Abstract

Results are reported from experiments, and numerical analysis of wake fields set up by electron bunches passing through a cylindrical dielectric liner made of alumina. The bunches excite many TM- modes, and the *Ez* component of wake field is sharply localized on the axis periodically behind the bunches. The experiment is at ATF Brookhaven, and uses up to three 50 MeV bunches spaced by one wake field period (*21* cm) to study the superposition of wake fields by measuring the energy loss of each bunch after it passes through the 53-cm long dielectric element. The millimeter-wave spectrum of radiation excited by the passage of bunches is of interest too. The numerical analysis was aimed not only to simulate the behaviour of our device, but in general to predict dielectric wake field accelerator (DWA) parameters. It is shown that one needs to match the radius of dielectric channel with the bunch longitudinal rms-length to achieve optimal performance.

INTRODUCTION

In a dielectric wake field accelerator, a dielectric loaded waveguide supports wake fields radiated by the passage of an electron bunch (e-bunch), which travels at a speed exceeding that of light in the structure. Our studies here relate to a cylindrical structure, consisting of a thick cylindrical shell of alumina (high dielectric constant $\kappa \sim$ 9.6) having a small bore hole (radius $A = 1.5$ mm) and an outer radius ($R = 1.9$ cm), all contained within a close-fitting conducting cylinder, which serves as a vacuum wall. The waveguide dimensions and dispersion free dielectric with large κ will favour the coherent superposition of many waveguide modes [1,2,3]. In this, we describe a multi-bunch experiment, with the purpose to measure the energy loss of a short drive bunch train. Very short bunches will be employed to favour wake fields of high amplitude, also shown by micrometer scale rectangular structures excited by fsec driving bunches [4,5].

A variety of numerical studies having to do with DWA performance is presented. We assume that the wake fields interact with Gaussian- shaped bunches (commonly produced by RF- guns) with the head- half width σ_1, tail half- width σ_2, and negligible (mostly) transversal features. If not specified otherwise, κ =9.65, $A = 1.5$ mm, $R= 1.931$ cm, $\sigma_1 = 1$ ps, $\sigma_2 = 2.5$ ps, initial energy = 50 MeV.

NUMERICAL STUDIES

Many recently conducted theoretical studies consider only the interaction between wake fields and infinitely thin electron bunches, but only by taking into account the real longitudinal features of an electron beam, can one predict the efficiency, energy spread, and acting accelerating gradient on a test bunch, which comes after the train of N driving bunches. Describing the wake fields inside of a circular waveguide through the decomposition into the normal eigen-modes [3], and advancing this approach toward computation of the energy exchange between electron bunches and the electromagnetic fields one finds that the power radiated by a train of e-bunches is:

$$P = \frac{Q_0^2 \cdot \beta \cdot c}{16\pi \cdot \varepsilon_0 \cdot A^2} \sum_m \left(\Omega_m \cdot \sum_{i,j} q_i \cdot q_j \cdot \cos\left(\frac{\omega_m \cdot (z_i - z_j)}{\beta \cdot c} \right) \right)$$

where Q_0 – reference charge; $q_i = Q_i/Q_0$ with Q_i - charge of ith bunch; ω_m – eigen frequencies of the structure;

$$\Omega_m = \frac{f_m^2(0)}{\alpha_m} \cdot \left((\Gamma_c^m)^2 + \left(\frac{\Gamma_s^m}{2} \right)^2 \right)$$

with f_m – eigen functions, α_m – normalization coefficients, and Γ_c^m, Γ_s^m are given by:

$$\Gamma_c^m = \frac{\sigma_1}{\sigma_1 + \sigma_2} \exp\left(-\left(\frac{\omega_m \cdot \sigma_1}{2 \cdot \beta \cdot c}\right)^2\right) + \frac{\sigma_2}{\sigma_1 + \sigma_2} \exp\left(-\left(\frac{\omega_m \cdot \sigma_2}{2 \cdot \beta \cdot c}\right)^2\right)$$

$$\Gamma_s^m = \frac{\sigma_1}{\sigma_1 + \sigma_2} \exp\left(-\left(\frac{\omega_m \cdot \sigma_1}{2 \cdot \beta \cdot c}\right)^2\right) - \frac{\sigma_2}{\sigma_1 + \sigma_2} \exp\left(-\left(\frac{\omega_m \cdot \sigma_2}{2 \cdot \beta \cdot c}\right)^2\right)$$

Every bunch is located along the z- axis at z_i, moves at the speed of $\beta \cdot c$, and has the same shape, but different charge.

Deploying this expression for the case where the first N- bunches, spaced at $z_i = L \cdot (1-i)$, pump energy into the wake, and the very last bunch, located at $z_T = L \cdot (1-N-1/2)$ is accelerated, one derives the expressions for the set of parameters which should be used to describe a wake field apparatus as an accelerator device (L = wake field period):

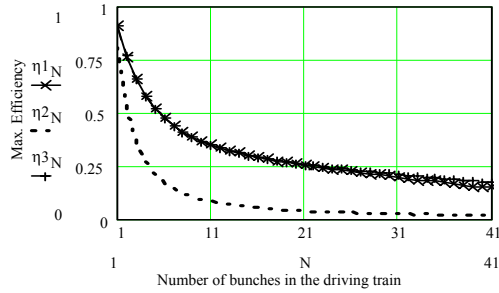- enhancement of the wake field due to its amplification by the train of N bunches:

$$\xi = \left(\sum_{m,i,j}^{\infty,N,N} \Omega_m \cdot \cos\left(\frac{\omega_m \cdot L \cdot (i-j)}{\beta \cdot c}\right) \right) / \sum_m^{\infty} \Omega_m$$
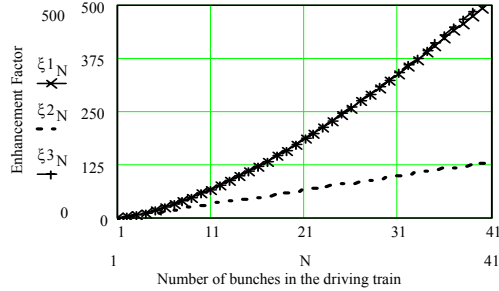
- structural ratio (we are introducing now as)

$$\chi_\rho = -\left(\sum_m \Omega_m \cdot \sum_i^N \cos\left(\frac{\omega_m \cdot L(N-i+1/2)}{\beta \cdot c}\right) \right) / \sum_m \Omega_m$$
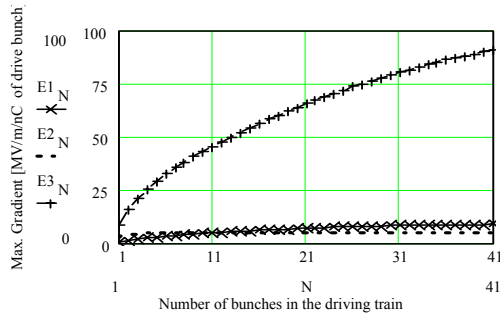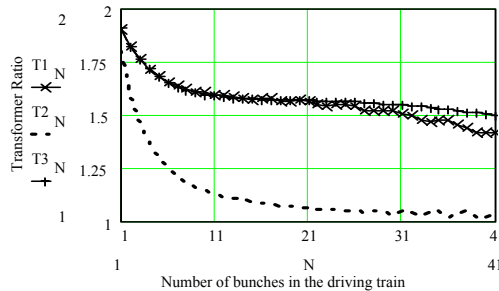
a) maximum possible accelerating gradient acting on a test bunch (given per [nC] of a driving bunch); the upper ($E3_N$) curve corresponds to the narrow bunch + small channel radius in the dielectric slab

b) maximum possible efficiency of energy transfer

c) enhancement of the wake field due to its coherent amplification by the train of N bunches

d) transformer ratio

Figure 1: Parameters of DWA are shown for the different bunch length and dielectric hole radius (σ_1, σ_2, A).
#1 – (1 ps, 2.5 ps, 1.5 mm) – solid, marked by "X",
#2 – (1 ps, 2.5 ps, 0.5 mm) – "dot",
#3 – (0.33 ps, 0.83 ps, 0.5 mm) – "dash", marked by "+"

- efficiency of energy transfer from the N- bunch train to a test bunch of charge $Q_T = q_T \cdot Q_0$

$$\eta = \frac{2 \cdot q_T \cdot \chi_\rho - q_T^2}{\xi}$$

with its maximum value of

$$\eta_{MAX} = \frac{\chi_\rho^2}{\xi}$$

- acceleration gradient acting on the test bunch:

$$E_T = \frac{Q_0}{16 \cdot \pi \cdot \varepsilon_0 \cdot A^2} \sum_m \Omega_m \cdot \left(2 \cdot \chi_\rho - q_T\right)$$

- customarily used transformer ratio [2] is expressed as:

$$TR_N = 2 \cdot \eta_{MAX} \frac{N}{\chi_\rho}$$

One sees that maximum efficiency occurs when a test charge equals χ_ρ, while the accelerating gradient drops down by 2 times from its possible maximum. Only a test charge less than $2 \cdot \chi_\rho$ can experience acceleration.

Fig. 1 gives examples of performances for several cases. The maximum gradient of 256 MV/m will be achieved after 20 narrow driving bunches each with charge $Q_0 = 4$ nC (see the #3 case.) One can increase significantly the accelerating gradient by reducing the channel radius in a dielectric only if it is accompanied by bunch shortening. The reason for this is that both the wake field peak where acceleration/ deceleration occurs and an e-bunch are features of almost the same longitudinal dimensions. When one reduces the channel radius the wake field can become narrower than the bunch, which leads to reduction of all performances (see the case #2 in Fig. 1, b), c), d). Fig. 2 demonstrates that when mismatching between the bunch length and the channel radius happens, almost all driving bunches (N≥ 4) cannot lose energy above some limit.
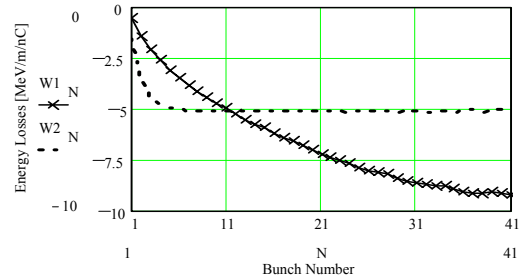

Figure 2: Energy lost by every consecutive driving bunch for different (σ_1, σ_2, A):
#1 – (1 ps, 2.5 ps, 1.5 mm) – solid, marked by "X";
#2 – (1 ps, 2.5 ps, 0.5 mm) – "dot"

In considering narrowing the driving bunches to improve performance, one should keep in mind that excessive narrowing may lead to an increment in the test bunch energy spread when a few drive bunches are used. The only reliable way to prevent it is to narrow the test

bunch. For drive $(\sigma_1, \sigma_2) \approx$ (1 ps; 2.5ps), and test $(\sigma_1, \sigma_2) \approx$ (0.3 ps; 0.8ps) the energy spread does not exceed 15 %.

The accuracy of bunch spacing (between any bunch and the reference bunch) must be better than 425 μm to avoid any performance decrease larger than 15 %. This also means that our model is valid when the time slippage of a bunch is within this range after interaction with the wake field. Thus, the DWA length must not exceed some limit, or, equivalently the acceleration gradient should be sufficiently high.

The Tab. 1 shows the lowest limit on gradient $E_{lim,min}$ when one plans to have gross energy losses/gain of W.

Table 1: Lowest gradient vs. planned energy gain/losses to use this numerical model

W [MeV]	0.1	1	10	50
$E_{lim,min}$ [KV/m]	0.05	4.8	375	4600

For the structure at ATF- BNL with the drive $(\sigma_1, \sigma_2) \approx$(1ps; 2.5 ps), Q0 $\approx$300 pC the decelerating/accelerating gradient is at least 500 times larger than the limit. The energy losses are: 1st bunch – 78; 2nd – 212; and 3rd – 315 KeV. The maximum accelerating gradient is 716 KV/m (after N= 3 drive bunches), and the acting gradient on a test charge of 150 pC will be 537 KV/m.

Should another set of $(\sigma_1, \sigma_2, Q_0, \kappa, A,$ etc) occur, the model allows the "quick-to-predict" computation of energy losses/gains and any other relevant parameters (ξ, η, E_T, etc)

EXPERIMENTAL STUDIES

Oversize alumina castings were obtained from LSP Industrial Ceramics (Lambertville, NJ). Since no sample 53 cm in length had the straightness of bore hole that was required, it was decided to use two selected shorter sections smoothly butted together and fitted into a metal-walled cylindrical vacuum jacket and waveguide. Initial measurements of the spectrum of TM_{0n} modes (after a single bunch) were made on a slightly oversized sample [6], which was then ground to the correct dimension (Fig. 3) for this experiment. A new measurement (Tab. 2) of the TM_{0N} frequencies shows that the wake field period is 21 cm.

The apparatus is installed on the 2nd beamline of the ATF- BNL, which was redesigned to meet the experimental (Fig. 4) requirements. New focusing triplets were introduced, together with beam profile monitors (BPMs) to produce the small e-beam transverse size and a suitable alignment to pass the bunch down the hole in the dielectric. The HeNe laser-and-optical system was employed to check the alignment on every assembling and operational step. The transport dynamics of the redesigned line has been studied intensely to insure matching between the ATF rf- linac and the apparatus.

The three driving bunches are obtained by splitting an optical pulse into three precisely delayed pulses, which impinge on the rf- photocathode gun within 30° of the peaks of 2.8 GHz field to generate the compressed electron bunches that are suitable for the excitation of multiple TM- mode wake fields. The spacing between drive bunches (equal to the wake field period *L*) will be adjusted to maximize energy losses of every individual bunch. Since in this test experiment no large bunch charge is available, the energy losses can be comparable with the energy jitter of the diagnostic apparatus, and a technique is being developed to maintain the same energy over a significant period of time.
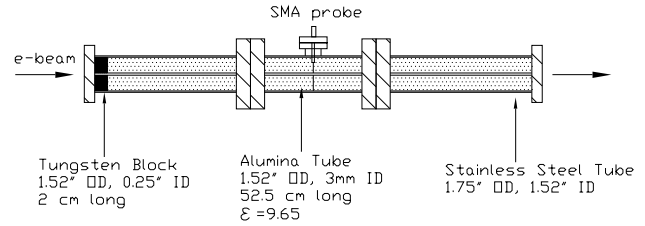

Figure 3: Apparatus drawing and dimensions

Table 2: Spectrum for $TM_{01} - TM_{06}$*

M#	1	2	3	4	5	6
Exp.	2.04	4.70	7.45	10.14	12.99	15.68
Th.	2.03	4.72	7.45	10.21	13.02	15.83

* *(frequencies in [GHz], M# - mode number, Exp. – experimental data, Th. – theoretical prediction ± 1% which results from κ =9.65 + 1%, R= 19.31 mm ± 0.3%, A= 1.5 mm ± 1%·R (the best manufacturing accuracy)*
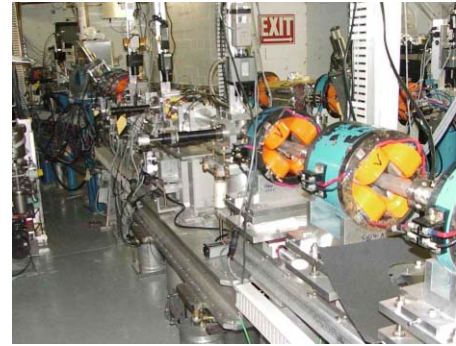

Figure 4: DWA experiment at ATF

REFERENCES

[1] T.B. Zhang et al, Physical Rev. E56, 4647 (1997).
[2] J.G. Power et al, PRST AB 3, 10132 (2000).
[3] S.Y. Park, J.L. Hirshfield, Physical Rev. E62, 1266 (2000).
[4] T.C. Marshall et al, PRST – Accelerators and Beams 4, 121301 (2002).
[5] T.C. Marshall et al., Advanced Accelerator Concepts Tenth Workshop, AIP Con. Proc. #647, p. 361.
[6] J.-M. Fang et al., Proc. of the PAC 1999, Vol. 5, p. 3627 (1999).

NUMERICAL STUDY OF INTERFERENCE BETWEEN TRANSITION RADIATION AND CERENKOV WAKE FIELD RADIATION IN A PLANAR DIELECTRIC STRUCTURE*

J.-M. Fang[†], T.C. Marshall, Columbia University, New York, NY, USA
V.P. Tarakanov, ITES, RAS, Moscow, Russia
J.L. Hirshfield, Yale University and Omega-P Inc, New Haven, CT, USA

Abstract

The PIC code KARAT is used to study the interference between transition radiation and Cerenkov wake field radiation, set up by the passage of a bunch of charge through a dielectric structure of finite length. An example studied is a tall, dielectric-lined rectangular wake field microstructure, recently proposed as a stageable element of an advanced linear accelerator, which would use a train of femtosecond duration bunches. These bunches would be chopped out of a longer bunch using a powerful CO_2 laser and formed into a rectangular-profile bunch by a quadrupole. The bunches set up a periodic wake field which can be built up to as much as 600 MV/m using ten 3-fs bunches each containing a charge of 1-pC. Of interest is the difference in relative propagation speeds of the transition radiation and the Cerenkov radiation (which advances almost at c), and the relative magnitudes of the fields.

INTRODUCTION

Acceleration of electrons in wake fields set up by a series of driving bunches in a dielectric structure has shown promise as a linear accelerator in which large gradient electric fields might be possible [1, 2]. Such wake fields are appealing because they do not require power injected into the structure from an external source, but rather use fields set up by bunches obtained from a conventional rf linac. Recently, we have studied the use of tall, planar dielectric wake field structures having micron-scale dimensions [3]. Such structures are capable of precision manufacture using microcircuit technologies, and have the capability of achieving very high field gradients: indeed, a series of ten, 3-fs, 1-pC charge bunches has recently been shown to set up a wake field of $\sim$ 600 MV/m in a structure 20 μm $\times$ 150 μm in cross section [4]. The bunches are 10 μm wide, and dielectric slabs a few μm thick line the structure (see Fig. 1). Planar dielectric structures offer the attraction of improving the stability of the bunch motion and the amount of charge carried compared with a cylindrical structure of comparable size, and the small transverse dimension permits a large wakefield to be developed.

The bunches could be obtained initially from a 500 MeV rf linac-type source, and are processed using a LACARA accelerator "chopper" [3], or possibly an IFEL [5] used as
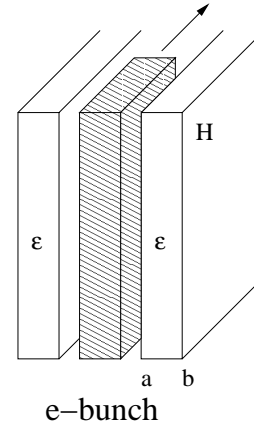
Figure 1: Schematic of slab bunch within a planar dielectric wake field structure.

a "pre-buncher", so as to obtain a sequence of bunches a few fsec in duration. A TW CO_2 laser is used as a "modulator" [3] of the original psec, nC bunch provided by the linac to form such a sequence of short bunches, periodically spaced, each having charge in the pC range. These *drive* bunches, the energy of which can be recycled, would be followed by an *accelerated* bunch which is situated in the accelerating component of E_z which follows the drive bunch train. In this way fields comparable with those achieved in laser plasma wake field accelerators can be set up, yet the energy is obtained largely from the rf linac source rather than a laser. We have found that it is possible to distort the original circular cross section of the input bunches into a near rectangular profile, using a quadrupole, and that the rectangular profile is maintained for a distance $>$ 10 cm of travel [3].

Transverse fields set up by the bunch have been calculated, and an estimate has been made of how far a drive bunch might travel without additional focusing [6] ($\sim$ 7.1 cm). Also, studies have been made of fields in 3D using the PIC code KARAT [7], and show that the E_z component of wake field is rather uniform across the structure. In the structure under study, the wake fields are dominated by two modes having nearly the same periodicity.
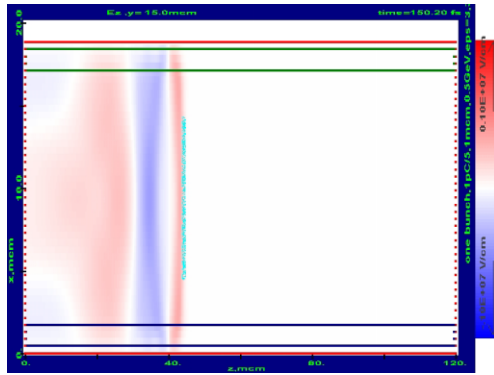
FIELDS FROM A SINGLE BUNCH

The transition radiation which is emitted when the bunch enters or leaves the structure is typically omitted in analytic

theoretical treatments of the wake fields. The transition radiation effect was remarked upon in [4, 8] and was recently treated analytically using a simplified model by Onishchenko, *et al* [9]. Qualitatively, the transition radiation emitted by the entry of the bunch into the structure interferes with the wake field radiation in a certain region. This region extends from the point where the bunch enters the structure to a front which expands with the group velocity of waves in the structure. As the bunch and its wake field move with nearly the speed of light, the expanding region between the transition zone and the bunch fills with wake field radiation which resembles that emitted by the bunch in an infinitely long structure. However, the group velocity depends on the mode frequency, so in cases of multimode operation (see e.g. [8]) the transition radiation zone would not be very clear. It shows up more clearly in the example of wake field structures in which mainly one mode is excited [9], which is the case studied here. The planar dielectric structure studied here is 18.8 μm $\times$ 30 μm $\times$ 120 μm long. The dielectric slab is 1.9 μm in thickness and has a dielectric constant ϵ of 3. The vacumn channel is 15 μm wide. The microbunch has a charge of 0.2-pC and its pulse duration is 3.3-fs long. The transverse profile of the bunch is 10 μm $\times$ 26 μm.

(a) at 150 femtosecond
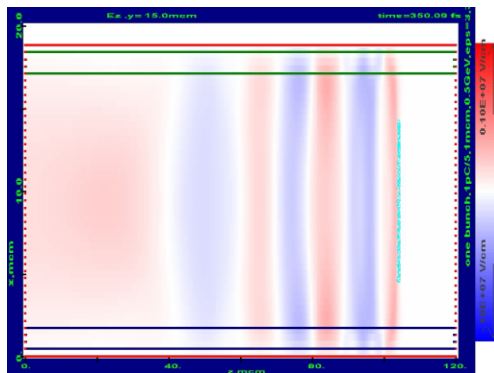
(b) at 350 femtosecond

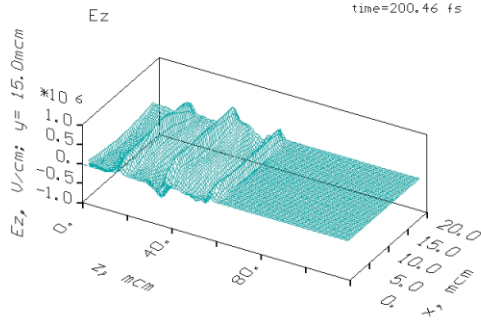Figure 2: Transition radiation and wake field from a single bunch.

Figure 2 shows the axial field E_z pattern in the x-z plane at the midway y-plane, at 150-fs and 350-fs after the en-

try of the first bunch into the structure. [These are color figures. The color scale indicates the magnitude of the field and the color itself represents the field's polarity (red for positive polarity and blue for negative).] The excited wake field alternates its polarity, thus the color in the figures too, periodically. In Fig. 2(a), the electron bunch has just entered the structure for a short period of time (150-fs), such that the transition radiation dominates and only one wake field period is seen following the electron bunch. As the electron bunch traverses into the structure further (Fig. (2b)), the wake field radiation pulls away from the transition radiation, due to the difference in their propagation speeds, and several wake field periods are formed. The period of the wake field is close to 20 μm. We also see the region where the transition radiation intereferes with the wake field radiation gradually expands, as the electron bunch propagates further. The propagation speed of the head of the wake field radiation is that of the bunch, whereas the propagation speed of the transition radiation front is estimated at about 1.7×10^{10} cm/sec, close to $c/\sqrt{\epsilon}$ (further study is needed to determine the propagation speed of the transition radiation). The magnitude of the wake field (E_z) is $\sim$ 40 MV/m, whereas the magnitude of the transition radiation is weaker, at $\sim$ 10 MV/m, an decrease which is consistent with the simplified analytic model by Onishchenko, *et al* [9].
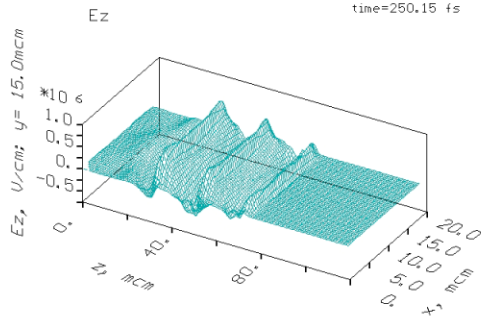
FIELDS FROM THREE BUNCHES

For the excitation of the wake field in a dielectric structure, a high gradient accelerating field can be obtained by using a train of bunches, carefully spaced at the wake field's period [1, 2].

For the dielectric structure in which mainly one mode is excited, transition radiation has an effect on the build-up of the wake field generated by a train of bunches. The dielectric structure we studied here is such a structure. For the PIC code Karat simulation, the bunches are placed 20 μm apart to match the wake field period of this planar structure and to permit the build-up of the wake field by coherent superposition. All other parameters are the same as the simulation for a single bunch. Figure 3 shows the axial field E_z in the x-z plane at mid y-plane at 200-fs and 250-fs. The build-up of the wake field is evidenced for the first 2 bunches of Fig. 3(a). The third bunch in Fig. 3(a), is still in the transition radiation zone and the wake fields of the three bunches don't add up linearly because of the interference between the transition radiation and the Cerenkov wake field radiation. As the bunches advance further away from the transition radiation region (Fig. (3b)), the build-up of the wake field is evidenced for all three bunches. Figure 4 is the E_z *vs* z plot along the center of the planar structure and gives a clear reading of the magnitude of the wake field. The intereference effect of the transition radiation is clearly seen in Fig. 4(a), as the magnitude for 2nd and 3rd wake field is nearly the same.
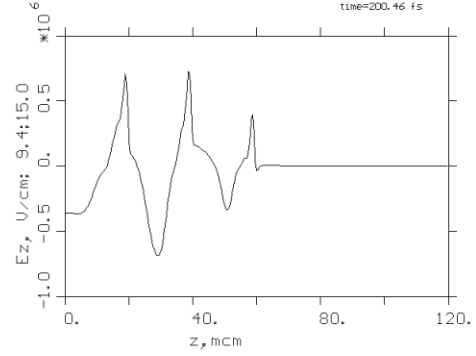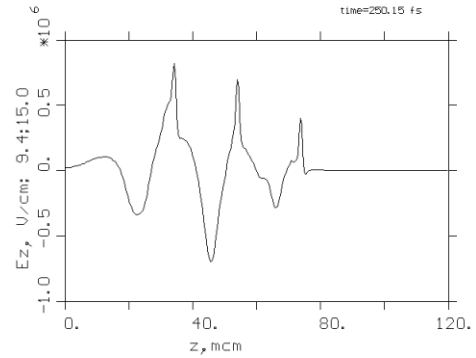
(a) 200 femtosecond

(a) 200 femtosecond

(b) 250 femtosecond

(b) 250 femtosecond

Figure 3: Transition radiation and wake field from three bunches.

Figure 4: E_z vs z along the center of the planar structure from three bunches.

CONCLUSIONS

We have studied the interference effect between the transition radiation and the Cerenkov wake field radiation in a planar dielectric structure using the PIC code Karat. We have chosen a structure where mainly one mode is excited. The transition radiation is important when the bunch has just entered the structure. Due to the difference in propagation speed between the transition radiation and the wake field radiation, a train of periodic wake fields is excited as the bunch advances further into the structure. The transition radiation also has an effect on the build-up of the wake field by a train of bunches. This is a problem for system that uses a very long train of drive bunches to build up the accelerating wake field in a short structure [10].

REFERENCES

[1] T.-B. Zhang, J.L. Hirshfield, T.C. Marshall, and B. Hafezi, Phys. Rev. **E56**, 4647 [1997]

[2] J.G. Power, M.E. Conde, W. Gai, R. Konecny, P. Schoessow, and A.D. Kanareykin, Phys. Rev. ST AB **3**, 10132 [2000]

[3] T.C. Marshall, C. Wang, and J.L. Hirshfield, Phys. Rev. ST AB **4**, 121301 [2002]

[4] T.C. Marshall, J.-M. Fang, J.L. Hirshfield, C. Wang, V.P. Tarakanov, S-Y. Park, "Wake Fields Excited in a Micron-Scale Dielectric Rectangular Structure by a Train of Femtosecond Bunches", p. 361, AIP Conference Proceedings **647** [2002]

[5] Y. Liu, et al., Phys. Rev. Lett. **80**, 4418 [1998].

[6] S-Y. Park, C. Wang, and J.L. Hirshfield, "Theory for Wake Fields and Bunch Stability in Planar Dielectric Structures", p. 527, AIP Conference Proceedings **647** [2002]

[7] V.P. Tarakanov, "Users' Manual for Code KARAT", BRA Inc., VA, USA [1992]

[8] T.C. Marshall, J.-M. Fang, J.L. Hirshfield and S-Y. Park, "Multi-mode, Multibunch Dielectric Wake Field Resonator Accelerator", p. 316, AIP Conference Proceedings **569**, [2000]

[9] Onishchenko, I.N., Sidorenko, D. Yu, and Sotnikov, G. V., Phys. Rev. **E65**, 066501 [2002]

[10] Onishchenko, I.N., Sidorenko, D. Yu, and Sotnikov, G. V., Ukrainian Physical J. **48**, 17 [2003]

Strong wakefields generated by a train of femtosecond bunches in a planar dielectric microstructure

Changbiao Wang and J. L. Hirshfield*

Physics Department, Yale University, New Haven, Connecticut, USA 06520
and Omega-P, Inc., 199 Whitney Avenue, New Haven, Connecticut 06511, USA

J.-M. Fang and Thomas C. Marshall

Applied Physics Department, Columbia University, New York, New York 10027, USA
(Received 13 November 2003; published 27 May 2004)

A tall, dielectric-lined rectangular wakefield microstructure is analyzed as a possible element of an advanced linear wakefield accelerator. This accelerator would be driven by a train of fs electron microbunches that would be chopped out of a longer bunch using a powerful CO_2 laser and then formed into a train of rectangular-profile bunches using a quadrupole. The bunches set up a periodic wakefield in the microstructure that can be built up to 400–600 MV/m, for example, using a train of ten 3-fs 1-pC bunches. Two major issues are examined. First, interference is studied using the particle-in-cell code KARAT between transition radiation and Cerenkov wakefield radiation, both set up by the passage of a charge bunch through a dielectric structure of finite length. Of significance is the difference in propagation speeds of transition radiation and Cerenkov radiation (which travels almost at the vacuum light speed c) and the magnitude of the respective fields. Second, stability is examined for drive and accelerated bunches using computations of test particle orbits in the longitudinal and transverse wakefields excited by the drive bunches. It is found that nearly all test electrons in the drive bunches are confined within the structure for a travel distance of 30 cm or more, while test electrons located in an accelerated bunch can have stable motion over greater than 30 cm without passing through the structure walls.

I. INTRODUCTION

Acceleration of electrons in wakefields set up by a series of drive bunches in a dielectric structure has shown promise as the basis for a linear accelerator in which large acceleration gradients can be achieved [1,2]. This concept is attractive since it would not require rf power to be injected into the structure from an external source, but rather would use wakefields set up by injected bunches obtained from a conventional low energy rf linac. With the objective of realizing such an accelerator, we have recently studied wakefield generation and beam stability in tall, planar dielectric wakefield structures having micron-scale dimensions [3]. Such structures are capable of precision fabrication using microcircuit technologies and have the capability of achieving very high field gradients: indeed, analysis has recently shown that a series of ten, 3-fs 1-pC charge bunches can set up an accelerating wakefield of ~ 500 MV/m in a structure 18.8 μm $\times$ 150 μm in cross section [4]. The bunches in that example are 10 μm wide, and dielectric slabs a few μm thick line the structure. Planar dielectric structures offer the attraction of improving the stability of the bunch motion and increasing the amount of bunch charge [5], as compared to a cylindrical structure of comparable size. It

is the small transverse dimension of the structure that permits large wakefields to be generated.

The bunches could be obtained initially from a conventional (e.g., 500 MeV) rf linac and processed using a LACARA chopper [3], or possibly an IFEL [6] used as a prebuncher, so as to obtain a sequence of bunches, each a few fs in duration. A TW-level CO_2 laser would be used as a modulator [3] of the original ps, nC bunch provided by the linac to form such a sequence of short bunches, each having charge in the pC range. These drive bunches, which can in principle be recycled, would in practice be followed by an accelerated bunch that is situated in the accelerating phase of axial electric field E_z which trails the drive bunch train. In this way accelerating fields comparable with those achieved in laser plasma wakefield accelerators can be generated, yet the energy is obtained largely from the rf linac source rather than from a laser. We have found that it is possible to distort the original circular cross section of the drive bunches into a near-rectangular profile by shaping the beam stop and using a quadrupole lens following LACARA, and that the near-rectangular profile can be maintained for some distance of travel without significant deterioration due to finite beam emittance [4].

In practice, a dielectric-lined waveguide has finite length, and transition radiation will be generated when a charge bunch enters the waveguide. Interference between this transition radiation and Cerenkov wakefield

---

*Corresponding author.
Email address: jay.hirshfield@yale.edu

radiation was confirmed in a previous calculation [4]. But how in detail this interference affects the form of wakefields needs careful examination. Accordingly, the 3D particle-in-cell (PIC) code KARAT [7] has been used to reveal the evolution of Cerenkov radiation and transition radiation in a rectangular dielectric-lined waveguide. Three zones (transition radiation, interference, and Cerenkov radiation) are clearly identified. The Cerenkov radiation zone expands as the charge bunch advances, since, in general, transition radiation propagates more slowly than Cerenkov radiation.

Even though the planar structure analyzed in this paper is tall, it is not infinitely tall. Thus bunch stability differs from that in an idealized 2D structure where, in the limit of high beam energy, it has been shown than transverse wake forces can vanish [5]. Indeed, analysis shows that transverse wake forces decrease, as compared to longitudinal forces, as the structure height increases. However, for the range of parameters studied, transverse wake forces are not negligible and may cause the bunches to defocus and pass through the walls of a narrow structure. An estimate has been made of how far a drive bunch might travel under the influence of the transverse fields set up by the bunch without additional focusing [8], although this estimate needs to be refined by dynamical calculations. Theory developed by Park *et al.* [8] is employed here to investigate bunch stability using dynamical equations. In the structure under study, the wakefields are dominated by a few very closely spaced modes having wavelengths of approximately 21.2 μm. Our findings show that adequate stability of the drive bunches can be obtained by choosing a tall structure (300 μm), and that a certain group of test particles situated initially in a grid of loci within an accelerated bunch, as depicted in Fig. 1, can be accelerated for a distance of 1 m without external

FIG. 1.   Schematic slab bunch within a planar wakefield structure with a height of 2d, a channel width of 2a, and a dielectric slab thickness of (b-a). All circles stand for test particles in the (decelerated) drive bunch while only filled circles stand for test particles in the accelerated bunch.

focusing, maintaining a nearly stable profile and gaining an energy exceeding 550 MeV. This large magnitude of stable acceleration gradient motivates the analysis in this paper, so as to work towards realization of an advanced high-gradient linear accelerator based on the principles enunciated here.

II. TRANSITION RADIATION EFFECTS

The transition radiation that is emitted when the bunch enters or leaves the structure is typically omitted in analytic theoretical treatments of wakefields. The presence of transition radiation from entry and exit of a dielectric-lined structure was remarked upon in previous publications [4,9] and was recently treated analytically by Onishchenko *et al.* [10] using a simplified model. Qualitatively, transition radiation emitted by the entry of a bunch into the structure interferes with Cerenkov wakefield radiation in a certain zone. For the sake of convenience, three zones can be defined: the transition radiation zone where only the transition radiation dominates, the Cerenkov radiation zone where only the Cerenkov radiation dominates, and the interference zone where the two compete. The transition radiation zone plus the interference zone extends from the point where the bunch enters the structure to a front that expands with an effective group velocity of transition radiation waves in the structure. As the bunch and its wakefield move with nearly the speed of light, the expanding Cerenkov radiation zone between the interference zone and the bunch fills with wakefield radiation which resembles that emitted by the bunch in an infinitely long structure. But since the group velocity depends on the mode frequency, the transition radiation and interference zones would not be very distinct in cases of multimode operation (see, e.g., [9]). The respective zones are distinct in the example of wakefield structures in which only one mode is excited [10], which approximates the case studied here.

The first example of studies [4] described here of wakefields set up by a bunch entering a rectangular structure is for a structure with dimensions 2d = 150 μm, 2a = 15 μm, 2b = 18.8 μm, and dielectric constant ε_r = 3.0. The bunch height is also 150 μm, while the width is 10 μm and the length is 1 μm; the bunch charge is 1 pC and its energy is 500 MeV. The motion of the bunch was followed for 60 μm, and an axial field intensity contour plot in the *z-x* plane is presented in Fig. 2. Following the bunch (located but not shown at the right-hand side at z = 60 μm) is seen one complete wakefield period of E_z; to the left of that ($z < 30$ μm) the field structure is more complex. This is the zone where transition radiation appears. However, one finds that wakefield radiation by itself is quite uniform over the *x-y* plane for this choice of parameters, as shown in Fig. 3, showing that near its center a tall rectangular structure can be approximated by
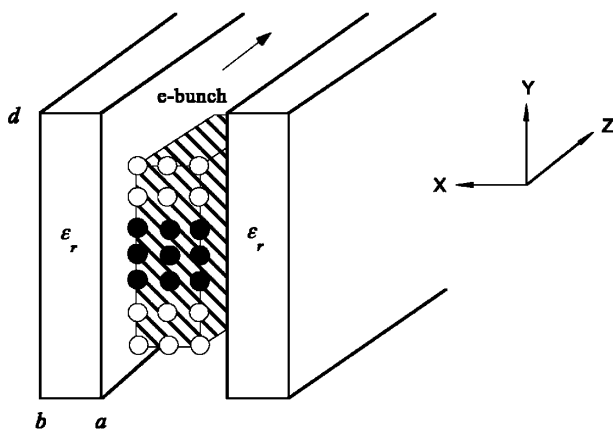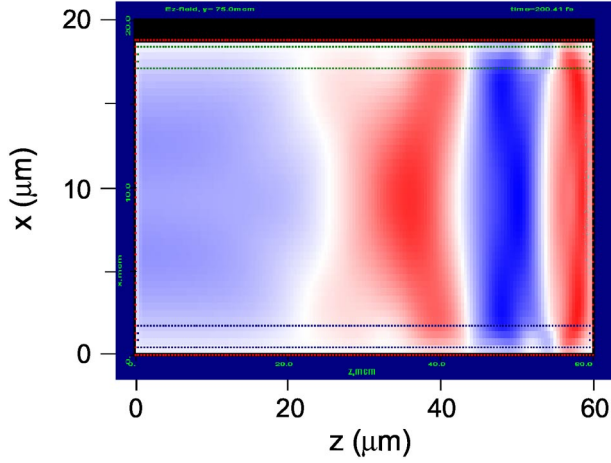
FIG. 2. (Color) Wakefield from a single bunch (located at $z = 60$ μm), moving to the right, shown in the z-x plane at a y-plane location halfway between the top and the bottom. The dielectric boundaries are the horizontal lines at $x = 1.9$ and 16.9 μm. The color scale on the right is proportional to the field intensity, and the maximum is ± 40 MV/m in magnitude. Note the diffuse region for $z < 30$ μm due to the interference of the wakefield and transition radiation.

FIG. 3. (Color) Wakefield in the x-y plane at $z = 51$ μm. The moving bunch is located at $z = 60$ μm. The vertical and horizontal scales are not the same: 150 μm tall by 18.8 μm wide. Note the field is nearly uniform except for around the two y ends. The dielectric boundaries are shown as vertical lines on the left and the right.

its 2D counterpart. The maximum axial field from this single bunch is about 40 MV/m.

In order to follow the development of the transition radiation interference pattern further using KARAT, it was necessary to reduce the bunch height to 30 μm and the bunch charge proportionately, so as to work within the available computer capabilities. This choice introduces

3D features into the wakefield pattern, but if we examine the axial electric field at $y = 0$, we can get a good understanding of how these fields evolve. This is shown in Figs. 4 and 5, after the bunch has traveled first 150 fs (45 μm, Fig. 4) and then 350 fs (105 μm, Fig. 5) from the point of entry on the left. The interference zone where transition radiation interferes with wakefield radiation moves more slowly than the wakefield radiation itself, which follows the bunch at the bunch speed ($\sim c$). Thus as the bunch moves along the structure, the Cerenkov
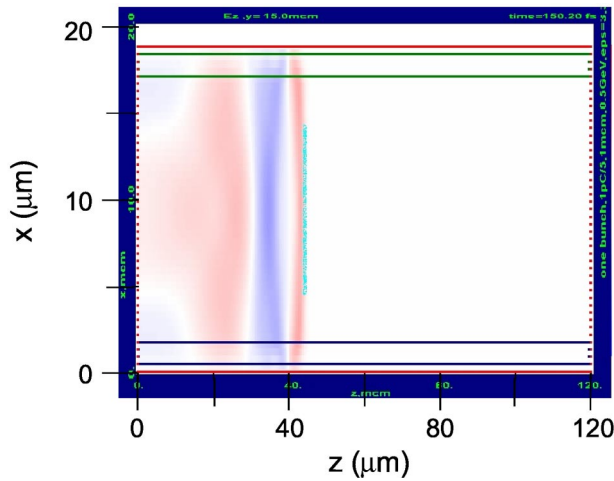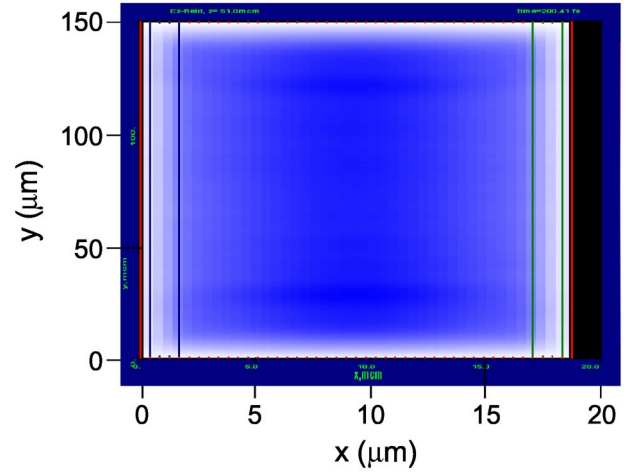

FIG. 4. (Color) Pattern of axial electric field, shown in the z-x plane at midplane $y = 0$ when a bunch has traveled 150 fs from the point of entry on the left. Since the transition radiation is weaker and the Cerenkov radiation has periodicity, the three regions can be approximately distinguished: transition radiation region ($z < 13$ μm), interference region ($13 < z < 26$ μm), and Cerenkov radiation region ($26 < z < 45$ μm). In this figure, the total axial length is 120 μm.
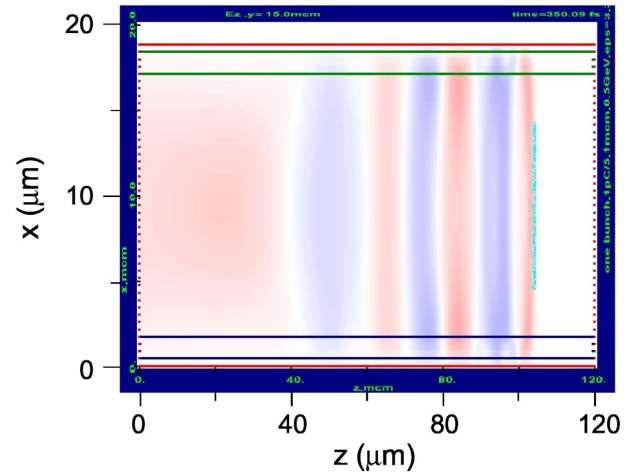

FIG. 5. (Color) Pattern when the bunch has traveled 350 fs from the point of entry on the left. It is seen that all the transition radiation region ($z < 40$ μm), the interference region ($40 < z < 60$ μm), and the Cerenkov radiation region ($60 < z < 105$ μm) have expanded, with the Cerenkov radiation region filled with more than two periods of wakefield radiation.
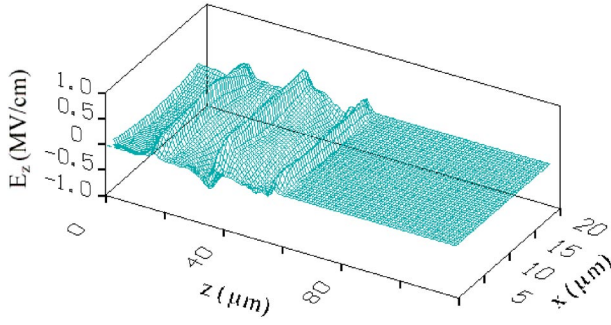
FIG. 6. (Color) Superposition of axial field E_z excited by three individual bunches in the z-x plane at the midplane $y = 0$ at 200 fs after entry of the first bunch into the structure. The third bunch still is in the transition zone and the fields of the three bunches do not add up at the third bunch position.

radiation zone between the interference zone and the bunch expands and fills with periodic (~ 20 μm) wakefield radiation, just as would be predicted by overlooking transition radiation. In this example, the boundary between the Cerenkov radiation zone and the interference zone appears to move at about 1.7×10^{10} cm/s, close to $c/\varepsilon_r^{1/2}$. The magnitude of the interference radiation, about 10 MV/m, is consistent with that obtained in the simplified analytic model of Onishchenko *et al.* [10].

A high-gradient accelerating field can be obtained by using a train of bunches, carefully spaced by the wakefield period so that constructive superposition of the wakefields of the individual bunches occurs [1]. In this case as well, transition radiation has an effect on the superposition. We demonstrate this by modeling a train of three drive bunches placed one period apart; all other parameters are the same as above. Figures 6 and 7 show the axial field E_z in the x-z plane at the midplane $y = 0$ at 200 and 250 fs (60 and 75 μm) after entry of the first bunch into the structure. In Fig. 6 one sees the buildup of fields for the first two bunches. The third bunch is still in the transition zone and one can see that the fields of the three bunches do not add up linearly at the third bunch
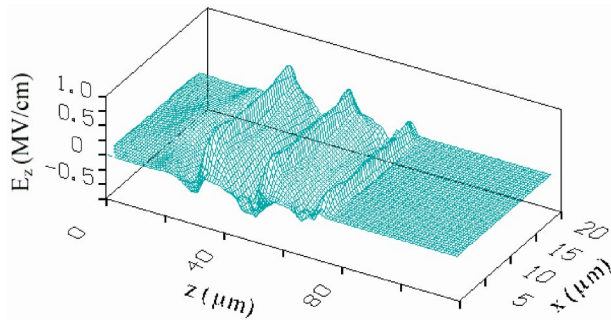

FIG. 7. (Color) Superposition of axial field E_z excited by the three bunches at 250 fs after entry of the first bunch into the structure. It is seen that the fields of the three bunches add at the third bunch position (see Fig. 9).
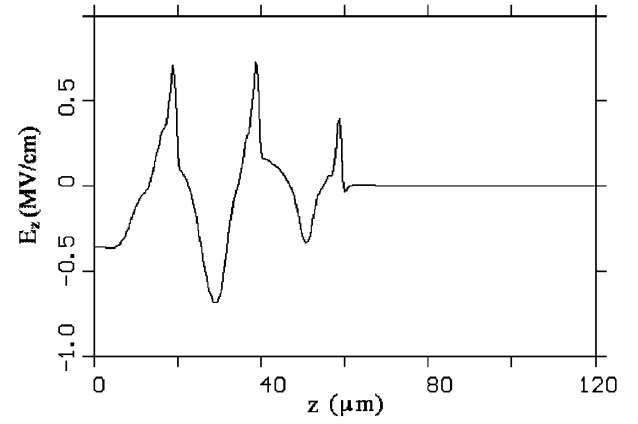

FIG. 8. Dependence of axial field E_z on axial distance z at $x = 0$ and $y = 0$ for Fig. 6. It is seen that the magnitudes of the electric field at the second and third drive bunch positions are the same.

position. A more quantitative rendering of this is shown in Fig. 8. The individual magnitudes of the electric field E_z of the second and third drive bunches are the same. As the bunches advance further (Figs. 7 and 9 at 250 fs), progressive buildup of the wakefields is obtained. These results suggest that transition radiation interference might well limit superposition of fields for a system that uses a very long train of drive bunches to build up the accelerating wakefield in a short structure [11].

III. STABILITY OF PARTICLE MOTION

A nonzero transverse gradient of E_z must result in variation of transverse wakefields with axial distance, following the Panofsky-Wenzel theorem. So although the E_z component can be nearly uniform in x and y at certain distances behind the drive bunch (see Fig. 3), bunch stability must be examined because even small transverse wakefields may cause the bunches to strike
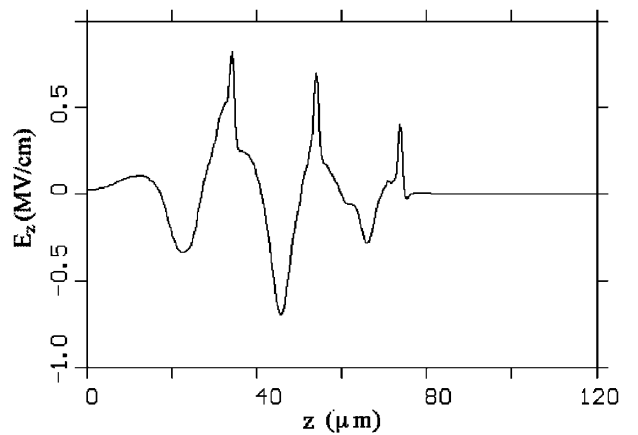

FIG. 9. Dependence of axial field E_z on axial distance z at $x = 0$ and $y = 0$ for Fig. 7. The electric field at the third bunch position is considerably stronger than at the second bunch.

and penetrate the walls of this small structure as they move along an axial distance of practical length. A complete theory for excitation of wakefields in 3D planar dielectric-lined structures, similar to the theory for cylindrical devices [12], has been formulated [8]. Park has also written a code [13] based on his theory to calculate distributions of wakefield forces excited by a train of rigid electron bunches moving at constant velocity. The code is used here to calculate dynamics for test particles by adding a routine that solves the Lorentz force equations, in which the wakefield forces are given as in Ref. [8]. All test particles are initialized to have the same velocity, and the effect of beam emittance is discussed in Sec. IV.

In this computation, the dimensions of the dielectric structure shown in Fig. 1 are taken to be $2d = 300$ μm, $2a = 15$ μm, and $(b - a) = 1.9$ μm, and again the dielectric constant ε_r is 3.0. For the distribution of charge within a bunch, we take a rectangular shape in the x and z directions, but choose a Gaussian profile for the y (tall) direction (see Appendix A). The bunches have an rms height of 70.7 μm, a width of 10 μm, and a length of 1 μm (3 fs), with each bunch containing 1 pC of charge, and the bunch centers are set on the axis of symmetry. The initial velocity of the test particles is taken to be the same as the drive bunch, which has a relativistic factor $\gamma = 1000$ (510.5 MeV). Self-field effects and the reaction of wakefields on the drive bunches are neglected. In the simulations, $11 \times 81 = 891$ computational particles situated initially in an x-y grid of loci were used to calculate the interaction between wakefields and test particles. The test particles in the drive bunch are initially distributed within a 10 μm $\times$ 159.2 μm rectangle, while the test particles in the accelerated bunch are located within a 10 μm $\times$ 31.8 μm rectangle.

The phase of injection of the accelerated bunch can be optimized. At a distance behind the last drive bunch appropriate for acceleration, the transverse wakefields are small while the axial field is large. Since the axial slippage between the wakefields and accelerated particles is negligible, one can estimate which wakefield peaks are potentially favorable for acceleration using the initial field distribution. Therefore, we first find the possible positions and then do dynamic simulations one by one to obtain the optimum injection location from the viewpoint of stability.

We begin by showing in Fig. 10 the amplitude spectrum of the modes excited by a single drive bunch. We observe that the spectrum is dominated by a few modes, having mode indices $n_x = 1$ and $n_y = 1$, 3, and 5, corresponding to wavelengths of 21.75, 21.56, and 21.19 μm. If the distribution of charge within the bunch were uniform, a broader spectrum of y eigenmodes would be excited, leading to the unfavorable effect of loss of bunch charge during the motion. Thus the optimum choice of the distribution and its height is that which retains the most
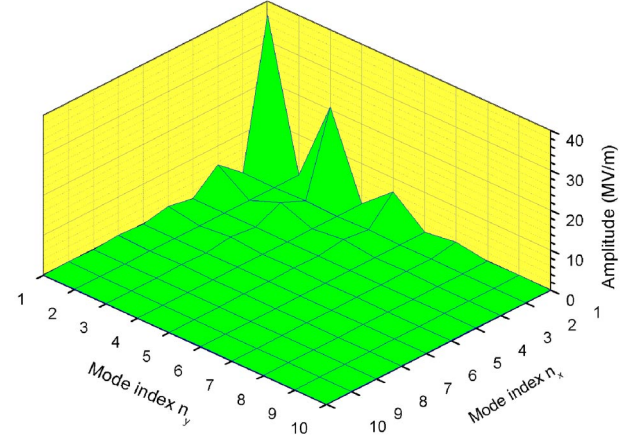

FIG. 10. (Color) Mode amplitude vs mode indices n_x and n_y for one drive bunch. It is seen that the modes with ($n_x = 1$, $n_y = 1$, 3, 5) corresponding to the wavelengths 21.75, 21.56, and 21.19 μm are dominant (36.6, 20.6, and 6.6 MV/m), and next the modes with ($n_x = 3$, $n_y = 1$, 3, 5) corresponding to the wavelengths 5.02, 5.01, and 5.00 μm are relatively weak (5.3, 3.1, and 1.0 MV/m). The modes with even n_y cannot be excited and those modes with $n_y > 10$ and $n_x > 5$ can be well ignored in computation.

charge as the drive bunches move along the device. The spectrum also shows us that the modes with $n_y > 10$ and $n_x > 5$ (all at short wavelengths less than 2.2 μm) can be safely ignored in computation since they are relatively weak (< 0.44 MV/m).

A. Motion of drive bunches

Coherent buildup of wakefields from successive drive bunches requires a fixed bunch spacing given by the wakefield period (21.2 μm). For this configuration, we provide in this section evidence of bunch stability by computing orbits of particles in the last bunch in a periodic bunch train, assuming that the preceding drive bunches are rigid. Of course, this assumption cannot give a complete understanding of stability for the entire bunch train. However, it does provide guidance, in that serious signs of instability and particle loss in this simple model would surely call into question the entire concept of using a train of drive bunches to build up a strong wakefield. In the example analyzed here, the first drive bunch is set at $z = 1200$ μm and the 10th drive bunch is at 1009.2 μm. The stability of the 10th drive bunch is examined by initially setting test particles at $z = 1009.2$ μm, where the axial wakefield force on the axis is nearly maximum, equal to -430.7 MeV/cm, as accumulated from the first nine drive bunches.

It is helpful to take a look at the configuration of wakefield forces to understand interactions between wakefields and test particles. The wakefield forces F_x, F_y, and F_z at $z = 1009.2$ μm are shown in Figs. 11–13. It is seen from Fig. 11 that F_x is antisymmetric with respect
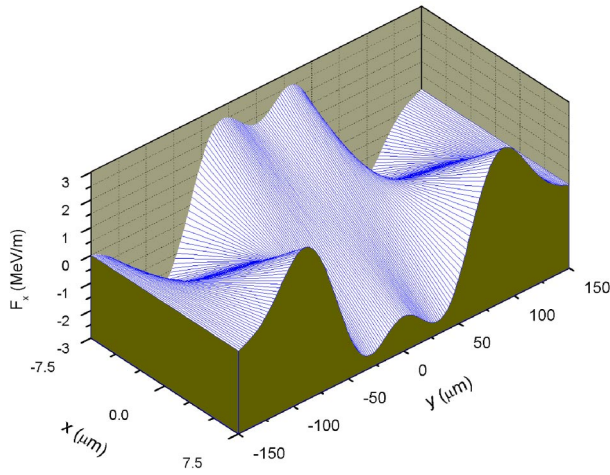
FIG. 11. (Color) Dependence of F_x on x and y at $z = 1009.2$ μm. F_x is focusing in the x direction when $xF_x < 0$, while F_x is defocusing when $xF_x > 0$. It is seen that F_x is focusing in the region: $-60.4 < y < 60.4$ μm, while defocusing in the two regions: $60.4 < |y| < 150$ μm.

to x and symmetric with respect to y. The magnitude of F_x increases nearly linearly with $|x|$, and F_x is either focusing or defocusing in the x direction, depending on y. F_x is focusing in the region: $-60.4 < y < 60.4$ μm, while defocusing in the two regions: $60.4 < |y| < 150$ μm, for example. F_y is symmetric with respect to x and antisymmetric with respect to y; it varies slowly with x while fluctuating up and down with y, as shown in Fig. 12. It is seen that $F_y < 0$ when $0 < y < 131.6$ μm; thus F_y is focusing in the y direction in the region of $|y| < 131.6$ μm. It follows from above that both F_x and F_y are focusing in the common region $|x| < 7.5$ μm and $|y| < 60.4$ μm. F_z is symmetric with respect to both x and y, as shown in Fig. 13. It is seen that F_z also varies slowly

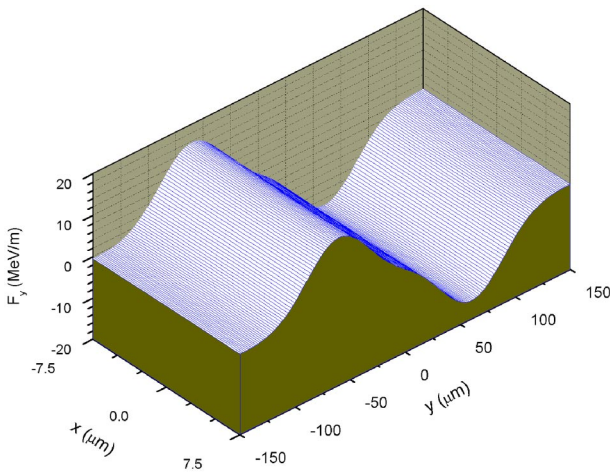FIG. 12. (Color) Dependence of F_y on x and y at $z = 1009.2$ μm. F_y is focusing in the y direction in the region of $|y| < 131.6$ μm, leading to a common region of $|x| < 7.5$ μm and $|y| < 60.4$ μm, where both F_x and F_y are focusing.
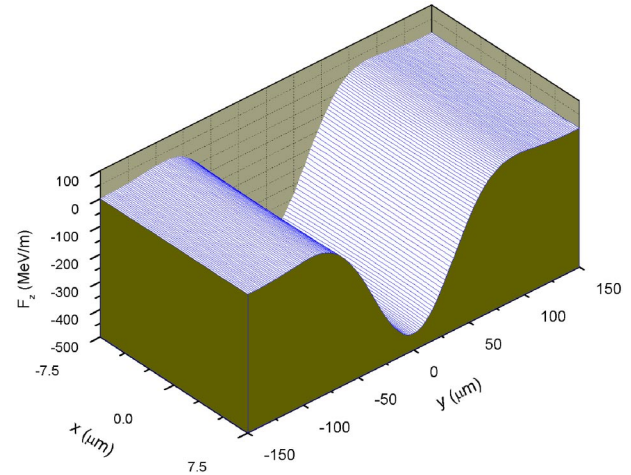

FIG. 13. (Color) Dependence of F_z on x and y at $z = 1009.2$ μm. It is seen that there is a small change in F_z in the x direction and a large change in the y direction. $F_z = -430.7$ MeV/m at $x = y = 0$.

with x from -430.7 MeV/m (at the center $x = 0$ and $y = 0$) to -441.1 MeV/m (at the edge $x = 7.5$ μm and $y = 0$), with only a 10.4 MeV/m difference. However, it varies greatly with y; from -430.7 MeV/m at the center to 16.8 MeV/m at $x = 0$ and $|y| = 94.5$ μm, with about a 447 MeV/m difference, for example.

Now consider the motion of test particles of the 10th drive bunch. Figure 14 shows the distributions of test particles at $z = 1009.2$ μm, 6 cm, 13.3 cm, 18 cm, 26 cm, and 30 cm under the influence of the wakefields. The test particles are initially distributed in the range extending from $x = -5$ μm to $+5$ μm and $y = -79.6$ μm to $+79.6$ μm, where the focusing $|F_x|$ takes maximum at $y = \pm 30$ μm and ripples as $|y|$ changes, while the focusing F_y changes little with x. Both the F_x and F_y focusings can be easily identified from the $z = 6$ cm distribution; the x dimension (width) is smallest at $y = \pm 5.5$ μm instead of ± 30 μm because of F_y focusing; the y dimension (height) varies little with x. It is seen from Fig. 14 that the particle distribution is changed considerably during the deceleration so that some particles get lost to walls. Figure 15 shows the dependence of the average relativistic energy factor and percentage of surviving particles as a function of axial distance. All the particles go ~4 cm without hitting any walls, and 93.7% arrive at $z = 30$ cm. The particles are decelerated from $\langle \gamma \rangle = 1000$ (510.5 MeV) to 789.7 (403.0 MeV), with 107.5 MeV lost to wakefields. The intensity of radiation generated from the ten drive bunches as they move 30 cm can be estimated from the energy losses to be 0.34 MW/cm^2, which is not a level which would be destructive for the dielectric material at these wavelengths.

Simulations show that 100% of the test particles in the second drive bunch survive traveling 30 cm, while 99.6%
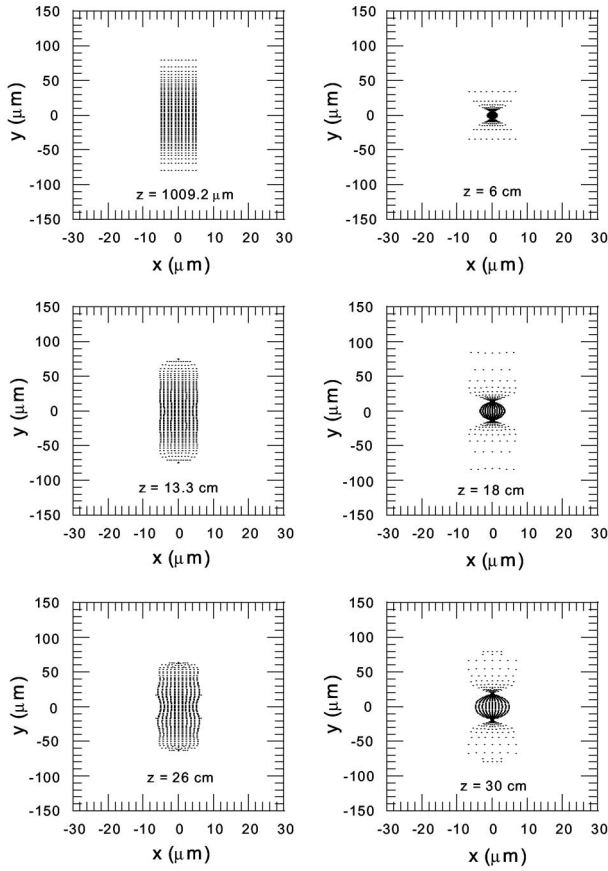
FIG. 14. Drive bunch test particle distribution at $z =$ 1009.2 μm, 6 cm, 13.3 cm, 18 cm, 26 cm, and 30 cm. The test particles are initially where the tenth drive bunch would be, preceded by nine actual rigid drive bunches. The initial distribution extends from $x = -5.0$ to 5.0 μm uniformly and from $y = -79.6$ to 79.6 μm Gaussianly. The F_x focusing and F_y focusing can be easily identified from the $z = 6$ cm distribution, and the distribution experiences focusing and defocusing alternatively.

survive at the fourth and 95.5% at the seventh. The percentage reduces with increase of the bunch sequence in all nine cases. These results help to justify the assumption that prior bunches are rigid, when examining the stability of a following bunch.

One can raise this question: Might a single drive bunch provide similar test particle acceleration and stability as does a train of bunches, providing the total charge is the same? Indeed, we find that the wakefield strength generated by and the stability of the test particles following a single bunch having the same charge as the total of the original bunches are comparable to the performance of the 10-bunch train. Nevertheless, it may be easier to generate a train of high quality, low charge, short bunches rather than a single drive bunch containing the combined charge. Also, the transition radiation loss emitted by a bunch as it enters or leaves the dielectric structure module scales as the square of the bunch charge, which favors greatly the train of smaller-charge bunches.
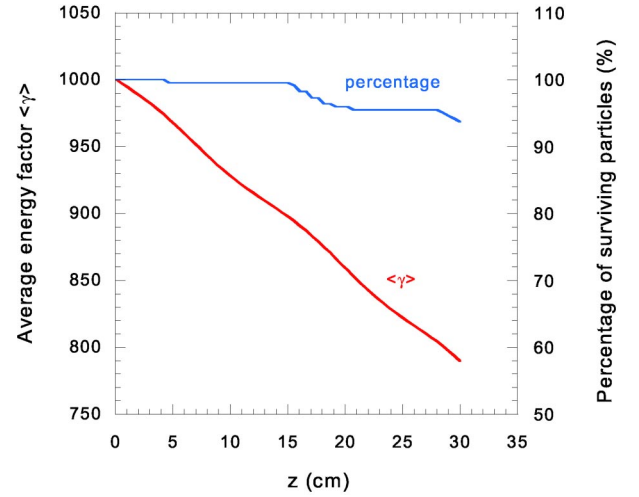

FIG. 15. (Color) Dependence of average energy factor $\langle\gamma\rangle$ and percentage of surviving particles on axial distance z. 93.7% of the particles survive at $z = 30$ cm and they are decelerated from $\langle\gamma\rangle = 1000$ (510.5 MeV) to 789.7 (403.0 MeV), with 107.5 MeV lost to wakefields.

B. Motion of an accelerated bunch

An accelerated bunch can originate from a different source than the drive bunches, so its timing can be optimized. The stability of accelerated particles depends on positions in the wakefield and the size of the region the particles occupy. Simulations show that the test particles in an accelerated bunch following a train of ten drive bunches as described above should be situated at $z = 996$ μm, where the transverse wakefield forces F_x and F_y are small and focusing in a rectangular region of $|x| \leq 5$ μm and $|y| \leq 15.9$ μm, while the axial wakefield force F_z on the axis reaches its peak, namely, 554.0 MeV/m, as shown in Fig. 16.

The wakefield force configurations for F_x, F_y, and F_z at $z = 996$ μm are shown in Fig. 17. Their symmetries are the same as in Figs. 11–13. F_x varies nearly linearly with x and has zeros at $y = \pm 29.2$, ± 89.4, and ± 150 μm, where $F_x \equiv 0$; $xF_x < 0$ in the region of $|x| < 7.5$ μm and $|y| < 29.2$ μm and thus F_x is focusing. $F_y \equiv 0$ at $y = 0$ and it is monotone, decreasing with y through zero from $y = -29.2$ μm to $+29.2$ μm; $yF_y < 0$ and F_y is also focusing in this region. F_z increases slowly with x from center to edge: $F_z = 554.0$ MeV/m at $x = 0$ and $y = 0$, while $F_z = 563.6$ MeV/m at $x = 7.5$ μm and $y = 0$. F_z decreases with y away from the center, with $F_z = 424.5$ MeV/m at $x = 0$ and $y = 29.2$ μm, leading to a force difference of 139.1 MeV/m in the region mentioned above. The force difference may cause energy spread for an accelerated beam. Therefore the acceleration test particles are localized in a smaller region of $|x| \leq 5$ μm and $|y| \leq 15.9$ μm to get better particle transmission, where the force difference is reduced to about 46 MeV/m.
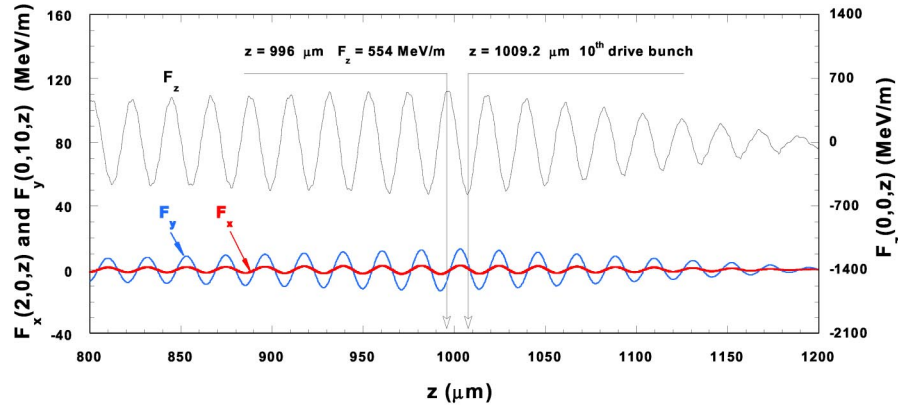
FIG. 16. (Color) Dependence of wakefield forces $F_x(2\ \mu m, 0, z)$, $F_y(0, 10\ \mu m, z)$, and $F_z(0, 0, z)$ on axial distance z, excited by ten drive bunches. The stability of the accelerated bunch is examined by setting test particles at $z = 996\ \mu m$ where $F_x = -1.4$ MeV/m and $F_y = -6.6$ MeV/m.

Figure 18 shows 3D orbits for 15 sampled accelerated particles initially uniformly distributed within a rectangle of $|x| \leq 5\ \mu m$ and $|y| \leq 15\ \mu m$ to show how the bunch profile changes as it moves along the axis; Fig. 19 shows distributions for 891 test particles on the x-y planes for different axial positions. It is seen that, during the course of acceleration, the particles experience focusing and defocusing alternatively, and they are all well confined within the beam channel over a 30-cm axial distance.

It is seen from Fig. 20 that the bunch of test particles is accelerated from $\langle \gamma \rangle = 1000$ (510.5 MeV) to 1322.3 (675.2 MeV) while traveling 30 cm, corresponding to an average acceleration gradient of 549 MV/m, with a final rms γ spread of 2.9 (1.5 MeV, or 0.22%). The acceleration energy increases linearly with axial distance while the energy spread goes up in a zigzag way. This behavior comes from the fact that around the focusing planes the bunch has a smaller cross section and the spread in wakefield acceleration force over the particles is also smaller, thus leading to a weaker increase of energy spread during that portion of the acceleration.

Simulations also show that about 95% of the test particles survive 100 cm travel; if the initial distribution area of test particles is reduced from 10 $\mu m \times 31.8\ \mu m$ to 10 $\mu m \times 17.5\ \mu m$, all the particles survive without hitting any walls and reach a final average acceleration energy of over 1 GeV ($\langle \gamma \rangle = 2081.0$).

IV. DISCUSSION

This paper discussed the interference between transition radiation and Cerenkov wakefield radiation in a tall, planar dielectric microstructure, using the PIC code KARAT. This study throws light on the use of wakefields to accelerate bunches of electrons. Formerly, analysis was confined to structures of infinite length, as the initial conditions near the entry of the bunch into the structure

were not treated. We have chosen conditions where mainly one wakefield mode is excited, and thus the physics is not complicated by multimode behavior. We find that because of the difference between the propagation speeds of wakefield radiation and transition radiation, a train of periodic wakefields still is excited behind the bunch as it advances into the structure. The amplitude of the transition radiation is smaller than the wakefield radiation [10], but it interferes with the latter in an expanding zone, and can affect the constructive superposition of wakefields from a train of following bunches. In general, transition radiation does not have the same periodicity as wakefield radiation, and therefore the interference can be destructive. Transition radiation also can be a problem for staged structures in a linear collider, because the radiation appears whenever a bunch enters or leaves a structure, and it is coherent in nature, scaling as the square of the bunch charge. By using many small bunches of charge to build up the wakefield, as we have done here, instead of one bunch of larger charge, the transition radiation energy loss is smaller, and thus more manageable.

We have used the motion of test particles to study the problem of stability of the driving as well as the accelerating bunches in the planar dielectric microstructure. The use of many small bunches of charge (in the pC range) in a structure having transverse dimensions of several μm results in very high wakefields being set up. The planar geometry also promotes exceptional stability, whereby the drive bunch train may move ~ 30 cm while losing a substantial fraction of its energy but only a small fraction of its initial charge. Furthermore, a carefully positioned bunch of accelerated particles can enjoy stable high-gradient acceleration for a distance ~ 1 m without the use of external focusing or guiding: a remarkable result, in view of the very small transverse dimensions of the structure. Studies of stagability would involve recycling the energy of the original drive bunches while
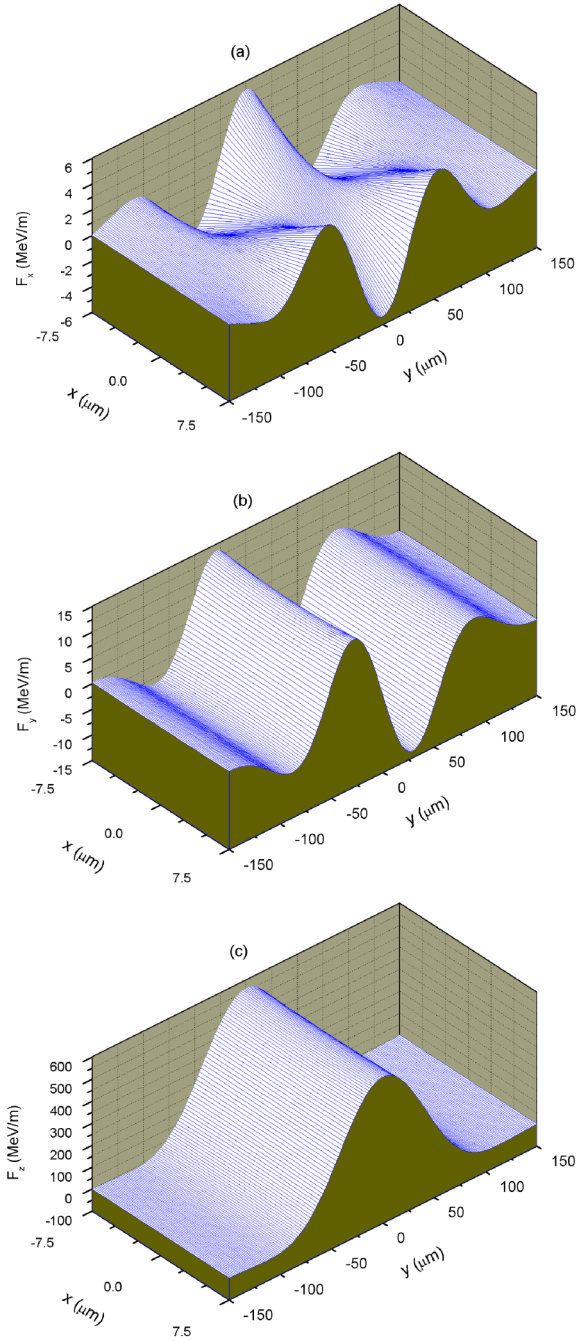
(a)

(b)

(c)

FIG. 17. (Color) Wakefield force configurations for (a). F_x, (b). F_y, (c). F_z at $z = 996$ μm. F_x and F_y are focusing in the region of $|x| < 7.5$ μm and $|y| < 29.2$ μm. The acceleration test particles are initially distributed within a rectangle of $|x| \leq 5$ μm and $|y| \leq 15.9$ μm, with F_z equal to 554.0 MeV/m at the center of $x = 0$ and $y = 0$.

FIG. 18. (Color) 3D orbits for 15 sampled accelerated particles initially distributed within a rectangle of $|x| \leq 5$ μm and $|y| \leq 15$ μm, with grid points of $x = -5$, 0, 5 μm and $y = -15$, -7.5, 0, 7.5, and 15 μm; six orbits initially at $y = \pm 15$ μm are marked with red, six orbits at $y = \pm 7.5$ μm are marked with blue, and three orbits at $y = 0$ are marked with black. Since $F_y(x, 0, z) = 0$ from Fig. 17(b), the three black orbits lie on the x-z plane. Similarly, $F_x(0, y, z) = 0$ from Fig. 17(a), and thus there are five orbits that lie on the y-z plane.

another set of drive bunches enters the next structure, followed by the original accelerated bunch; however, this problem has not been studied here.

This study of stability has used a very simplified model, in which the leading bunches do not change their shape or charge as the 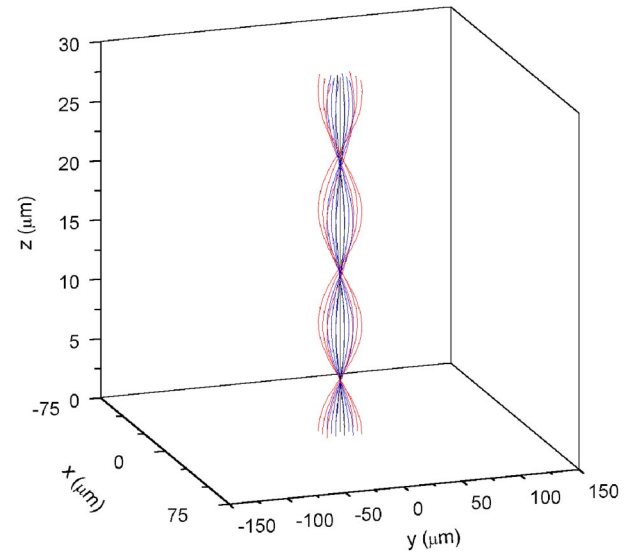motion proceeds. Actually, minor losses of charge have been shown to occur, as well as some distortion of bunch shape. However, to take these effects into account would involve a far more ambitious numerical study that is beyond the scope of this paper. Nevertheless, the remarkable stability found in our work strongly suggests that regimes of operation do exist wherein cumulative stability is found for a train of drive bunches and a following accelerated bunch.

Obtaining the results presented in this paper has required a certain amount of optimization. The choice of the bunch and structure heights, as well as the choice of the particle distribution in the bunch, was found to affect stability against transverse forces in substantial ways. For example, if the drive bunches were taken to be half the structure height with a uniform particle distribution, then acceptable travel distance without appreciable losses would be ~ 10 cm, which is a distance not only short of what would be an acceptable module length for a staged accelerator device, but also a distance too short to extract appreciable energy from these drive bunches. The bunch height can also exert an influence upon the stability results, as excitation of certain modes (e.g., $n_x = 1$ and $n_y = 7$) was found to be harmful for particle loss. A shorter bunch will excite more modes of the structure than will a taller one, and therefore its stability may be more difficult to assure.

As seen in Sec. III, the drive bunch centers are situated on the axis of symmetry of the structure; all the modes
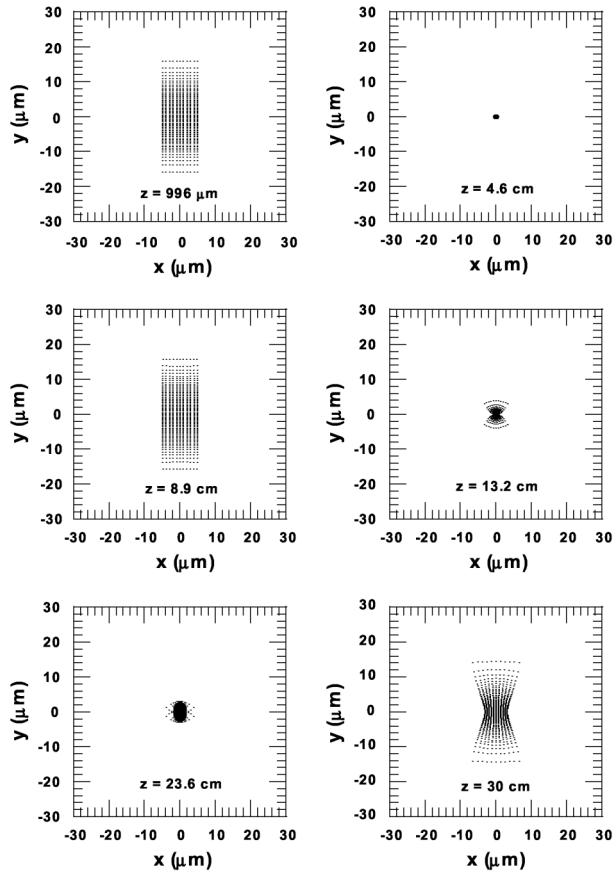
FIG. 19.   Acceleration test particle distributions on the *x-y* planes at $z = 996$ μm (initial), 4.6 cm (focusing), 8.9 cm (defocusing), 13.2 cm (focusing), 23.6 cm (focusing), and 30 cm (final). 891 electrons initially distributed uniformly in the *x* direction and Gaussianly in the *y* direction within a rectangle of $|x| \leq 5$ μm and $|y| \leq 15.9$ μm experience focusing and defocusing alternatively, and finally all the particles reach the end of $z = 30$ cm without hitting any walls.

with even index n_y (corresponding to those modes with E_z antisymmetric with respect to *y*) cannot be excited. If the bunch centers are set off the axis, those antisymmetric modes will be encountered, as indicated in a recent study [14] where a different approach is employed to obtain wakefields, avoiding need for a direct solution of Maxwell's equations [8]. The influence of antisymmetric modes on stability is a subject for future study.

A further simplification we have used has been the choice of zero emittance electron bunches and test particles. Stability and the small transverse dimensions motivate the use of 500 MeV bunches, which also will reduce the number of stages used in a high energy collider. Considering the smallest dimension of the system to be the 15 μm channel width, one can anticipate difficulties in obtaining the propagation of bunches over a 30 cm distance unless the emittance is sufficiently small. We have modeled the motion of a swarm of test particles located behind the ninth drive bunch, and from this we
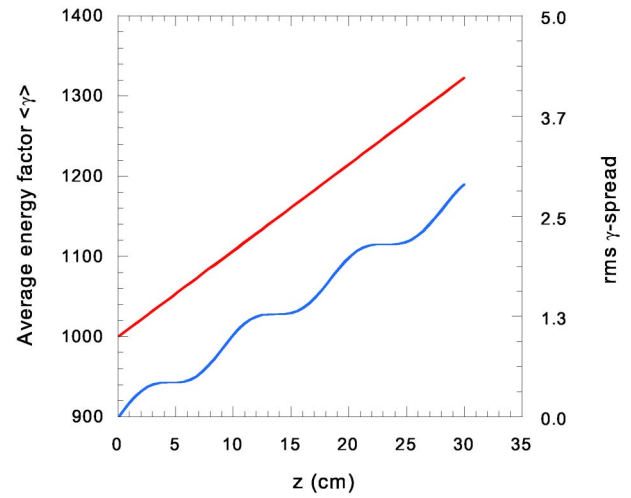

FIG. 20. (Color) Dependence of average energy factor $\langle \gamma \rangle$ and rms γ spread on axial distance *z*. The bunch of test particles is accelerated from $\langle \gamma \rangle = 1000$ (510.5 MeV) to 1322.3 (675.2 MeV) over a 30-cm distance, with an energy gain of 164.7 MeV and a final rms γ spread of 2.9 (1.5 MeV). It is seen that the energy spread increases much more slowly around the focusing planes ($z = 4.6$, 13.2, and 23.6 cm).

estimate that a normalized emittance of <0.5 mm mrad would be required to obtain satisfactory transmission of the drive bunch electrons as they move in the wakefields along 30 cm of axial travel. This requirement, which is sensitive to the profile of F_x in the region occupied by the test particles, is somewhat beyond the current state of the art (~ 1 mm mrad), but it is not unreasonable to hope for improvements of this magnitude in the future. For the accelerated electrons, small finite emittance is less important because the transverse forces are stronger there and are nearly linearly focusing in the entire region occupied by these particles; we find essentially zero losses of the accelerated test particles over 100 cm of travel using an emittance of 0.5 mm mrad. Nevertheless, a more sophisticated code is needed to better understand the effects of finite emittance in this problem.

We have not yet determined what the practical features of a possible staged high energy accelerator might involve, e.g., efficiency, alignment problems, etc. However, we have studied the suitability of dielectric structures which would have a similar performance as the one described herein but which have dimensions in the millimeter range. In order to obtain the same performance, the ratio of bunch charge to aperture area $Q/(4ad)$ must be kept the same, and the dispersion relation must yield a similar mode spectrum. As the latter requires that the dimensions must scale as the wakefield period, to construct a structure which would accept a train of bunches spaced by 9 mm would require a bunch charge which is ~160 nC, impractically large. This shows one advantage of working with a micrometer-scale structure.

We have chosen the wakefield period to be 21.2 μm here only for purposes of illustration. In practice, a choice of 10.6 μm might be advisable because the microbunches must be prepared using a laser. The dimensions of the planar dielectric device and the dielectric constant of the material would be chosen appropriately. A suitable dielectric material at 10.6 μm might be ZnSe (refractive index = 2.40), which can be formed by chemical vapor deposition [15]. This material is optically isotropic, has low losses in the far infrared, and is nearly free of dispersion.

Taken together, the results of this paper suggest that a high-gradient electron wakefield accelerator could be built with individual module lengths of 30–100 cm, wherein stable acceleration gradients of $\sim$0.5 GeV/m could be sustained using a train of drive bunches of charge only in the pC range.

APPENDIX A: INITIALIZATION OF A GAUSSIAN BEAM

In this Appendix, the procedure used for constructing a Gaussian distribution for computations presented in this paper is described. The Gaussian distribution in the y direction is assumed to be

$$f(y) = \frac{2}{\sqrt{\pi}\Delta y_0} e^{-[(y-y_0)/(\Delta y_0/2)]^2}, \tag{A1}$$

where y_0 is the bunch center. The rms height for this distribution is given by $2(\langle y^2 \rangle - \langle y \rangle^2)^{1/2} = \Delta y_0/\sqrt{2} = 70.7\ \mu$m if $\Delta y_0 = 100\ \mu$m, for example.

Suppose that there are N_y computational particles to be labeled in the y direction. The nth particle location b_n is implicitly given by the following equation:

$$\frac{2}{\sqrt{\pi}\Delta y_0} \int_{b_{n-1}}^{b_n} e^{-[(y'-y_0)/(\Delta y_0/2)]^2} dy' = \frac{1}{N_y+1}, \tag{A2}$$
$$(b_0 = -\infty, n = 1, 2, \ldots, N_y),$$

where the $(N_y + 1)$th or last particle is neglected in computations because it is represented as being at infinity.

Using the error function $\mathrm{erf}(x) \equiv (2/\sqrt{\pi}) \int_0^x e^{-t^2} dt$, we obtain from Eq. (A2)

$$\mathrm{erf}\left(\frac{b_n - y_0}{\Delta y_0/2}\right) - \mathrm{erf}\left(\frac{b_{n-1} - y_0}{\Delta y_0/2}\right) = \frac{2}{N_y+1}, \tag{A3}$$
$$(n = 1, 2, \ldots, N_y, \quad \text{and} \quad b_0 = -\infty).$$

Equation (A3) is a recurrence equation that gives locations of each of the N_y particles for the Gaussian distri-

bution Eq. (A1). The first computational particle at $y = b_1$ is a proxy for all the particles ranging from $-\infty$ to b_1 in the Gaussian distribution while that at $y = +\infty$ is a corresponding proxy for those ranging from b_{N_y} to $+\infty$. In the computations, those proxy particles are discarded, amounting to truncation of the Gaussian function. The fraction of particles truncated is $1/(N_y + 1)$. Obviously, accuracy in representing the Gaussian improves as N_y increases. For example, if $N_y = 81$, the truncated fraction is about 1.2%. In this case, the truncated representation for the Gaussian function is probably sufficient for purposes of this work.

[1] T.-B. Zhang, J. L. Hirshfield, T. C. Marshall, and B. Hafizi, Phys. Rev. E **56**, 4647 (1997).

[2] J. G. Power, M. E. Conde, W. Gai, R. Konecny, P. Schoessow, and A. D. Kanareykin, Phys. Rev. ST Accel. Beams **3**, 101302 (2000).

[3] T. C. Marshall, C. Wang, and J. L. Hirshfield, Phys. Rev. ST Accel. Beams **4**, 121301 (2002).

[4] T. C. Marshall, J.-M. Fang, J. L. Hirshfield, C. Wang, V. P. Tarakanov, and S. Y. Park, in *Advanced Accelerator Concepts: Tenth Workshop*, edited by C. E. Clayton and P. Muggli, AIP Conf. Proc. No. 647 (AIP, New York, 2002), p. 361.

[5] A. Tremaine, J. Rosenzweig, and P. Schoessow, Phys. Rev. E **56**, 7204 (1997).

[6] Y. Liu, X. J. Wang, D. B. Cline, M. Babzien, J. M. Fang, J. Gallardo, K. Kusche, I. Pogorelsky, J. Skaritka, and A. van Steenbergen, Phys. Rev. Lett. **80**, 4418 (1998).

[7] V. P. Tarakanov, computer code KARAT, BRA Inc., VA, USA, 1992.

[8] S.-Y. Park, C. Wang, and J. L. Hirshfield, in *Advanced Accelerator Concepts: Tenth Workshop*, edited by C. E. Clayton and P. Muggli (Ref. [4]), p. 527.

[9] T. C. Marshall, J.-M. Fang, J. L. Hirshfield, and S. Y. Park, in *Advanced Accelerator Concepts: Ninth Workshop*, edited by P. Colestock and S. Kelley, AIP Conf. Proc. No. 569 (AIP, New York, 2001), p. 316.

[10] I. N. Onishchenko, D. Yu. Sidorenko, and G. V. Sotnikov, Phys. Rev. E **65**, 066501 (2002).

[11] I. N. Onishchenko, D. Yu. Sidorenko, and G. V. Sotnikov, Ukr. J. Phys. **48**, 17 (2003).

[12] S.-Y. Park and J. L. Hirshfield, Phys. Rev. E **62**, 1266 (2000).

[13] S.-Y. Park (private communication).

[14] C. Jing, W. Liu, L. Xiao, W. Gai, and P. Schoessow, Phys. Rev. E **68**, 016502 (2003).

[15] D. N. Nikogosyan, *Properties of Optical and Laser-Related Materials: A Handbook* (John Wiley & Sons, New York, 1997), p. 286.